Impact of sample path smoothness on geotechnical reliability

Jianye Ching
Professor, Dept. of Civil Engineering, National Taiwan University, Taipei, Taiwan

Kok-Kwang Phoon
Professor, Dept. of Civil & Environmental Engineering, National University of Singapore, Singapore

ABSTRACT: The scale of fluctuation (SOF) of a spatially variable soil property has been known to be the most important parameter that characterizes the effect of spatial averaging, and the type of the auto-correlation model is thought to be of limited impact. This paper shows that this statement (SOF is the most important parameter) is true if the limit state function is completely governed by spatial averaging. However, this paper also shows that the sample path smoothness can have signifcant impact if the limit state function is not completely governed by spatial averaging. Three practical examples are presented to illustrate the effect of sample path smoothness.

In geotechnical engineering, the depth-dependent spatially variability $\varepsilon(z)$ is typically modeled as a zero-mean stationary random field with an auto-correlation function (ACF) $\rho(\Delta z)$ (Vanmarcke 1977, 1983) that defines the spatial correlation between two depths with Δz apart. The scale of fluctuation (SOF), denoted by δ, is defined to be the area under $\rho(\Delta z)$. Vanmarcke (1977) stated that the probability distribution of "point" soil properties may be less important, whereas the probability distribution of the "spatial averaged" soil properties is more relevant. The mean values for the point and spatially averaged properties are the same. The main difference between point and spatial average is that the latter has a smaller variance. The ratio between the spatial average variance and point variance is called the variance reduction factor. The effect of spatial averaging can be quantified by this variance reduction factor, because the mean value does not change. One important observation made by Vanmarcke (1977) is that the variance reduction factors for various ACF models (e.g., single exponential model (SExp), square exponential model (QExp), second order Markov model (SMK), etc.) do not differ significantly. If the limit state of a geotechnical problem is completely governed by spatial averaging, e.g., a friction pile under axial compression, Varmarcke's result suggests that design engineers should focus on the estimation of δ rather than the selection of the ACF model. In other words, it is expected that the failure probability of the friction pile does not significantly change if a different ACF model is adopted as long as δ remains constant.

It is less emphasized in the geotechnical literature that the random field sample paths obtained from different ACF models may have very different sample path appearances. Figure 1 shows two sample paths of a zero-mean random field with ACF models. All random fields have a unit SOF, i.e., $\delta = 1$. It is clear that for SExp, the sample paths are not smooth with significant local jitters, whereas the sample paths for QExp and SMK are smoother. The smoothness of random field sample paths is not an important factor if the only mechanism at play is spatial averaging. However, not many realistic problems have limit state functions completely governed by spatial averaging. The friction pile under axial compression is one well-known example that is completely governed by spatial averaging. In general, the limit state of a geotechnical structure can be governed by factors other than spatial averaging. For a limit state that is not completely governed by spatial averaging, it is of interest to

know whether SOF is still the only governing parameter. Three numerical examples will be adopted to address the research question. The first example is a friction pile under axial compression. The second example is an infinites slope with strength following a random field that varies in depth. The third example is a differential settlement problem.

1. WHITTLE-MATÉRN MODEL

The key issue is whether the sample path smoothness will affect reliability. The Whittle-Matérn (W-M) auto-correlation model (Stein 1999; Guttorp and Gneiting 2006; Liu et al. 2017; Ching et al. 2017a, 2017b) is a suitable ACF model that can produce random field sample paths with various degrees of smoothness in a controlled way. Its ACF model has the following format:

$$\rho(\Delta z) = \frac{2}{\Gamma(\nu)} \cdot \left(\frac{\sqrt{\pi} \cdot \Gamma(\nu + 0.5) \cdot |\Delta z|}{\Gamma(\nu) \cdot \delta} \right)^{\nu} K_{\nu} \left(\frac{2\sqrt{\pi} \cdot \Gamma(\nu + 0.5) \cdot |\Delta z|}{\Gamma(\nu) \cdot \delta} \right) \quad (1)$$

where ν is the smoothness parameter: sample paths of $\varepsilon(z)$ are ν-1 times differentiable with probability 1; Γ is the Gamma function (Abramowitz and Stegun 1970); K_ν is the modified Bessel function of the second kind with order ν (Abramowitz and Stegun 1970). Equation (1) is a two-parameter ACF. In contrast, the traditional ACF models such as SExp, QExp, and SMK are one-parameter models. The two parameters, ν and δ, can be independently selected to achieve a desired smoothness and scale of fluctuation. For $\nu = 0.5$ and ∞, the W-M auto-correlation model reduces to the SExp model and the QExp model, respectively (Rasmussen and Williams 2006). For $\nu = 1.5$, the W-M auto-correlation model reduces to the SMK model. The Fourier series method (FSM) (Jha and Ching 2012; Ching and Sung 2016) is adopted to simulate sample paths of $\varepsilon(z)$ based on the W-M model. Figure 1 shows some sample paths of $\varepsilon(z)$. The sample paths produced by the W-M model with $\nu < 1$ are not differentiable, e.g., when $\nu = 0.5$, there are significant local jitters.

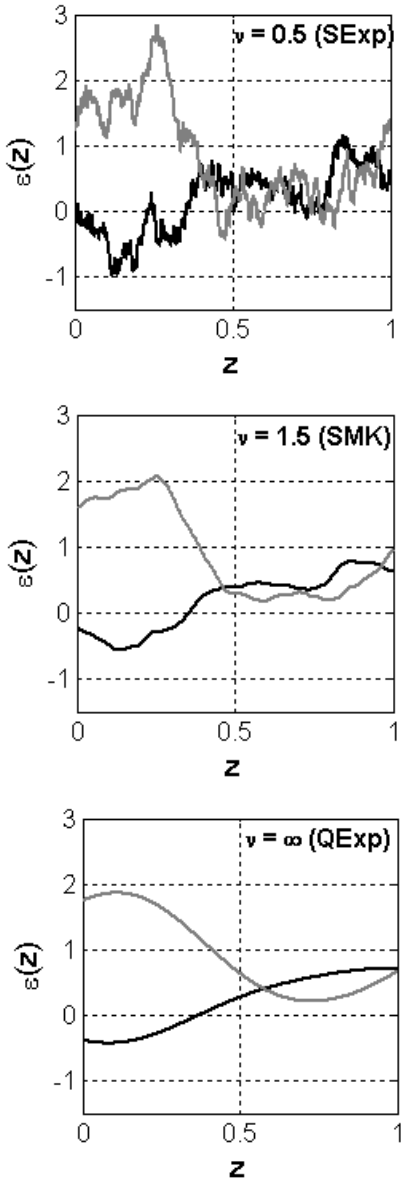

Figure 1 Some sample paths of $\varepsilon(z)$ produced by the W-M auto-correlation models with $\delta = 1$.

2. NUMERICAL EXAMPLES

Three examples are considered: (a) a friction pile under axial compression; (b) an infinite slope; and (c) differential settlement between two footings. The limit state for the first example is completely governed by spatial averaging. The limit state for the second example is not entirely governed by spatial averaging and is affected by the weakest-

path seeking mechanism. The limit state for the third example is not governed by spatial averaging as well.

2.1. Friction pile under axial compression

Consider a friction pile embedded in clay with a total length L = 10 m, subjected to an axial compression dead load DL = 1400 kN. The pile has a diameter B = 1 m. The spatially variable undrained shear strength (s_u) of the clay is modeled as a stationary normal random with mean μ = 100 kN/m^2 and coefficient of variation (COV = standard deviation/mean) = 30%:

$$s_u(z) = \mu + \sigma \cdot \varepsilon(z) \quad (2)$$

where σ = 30 kN/m^2 is the standard deviation of $s_u(z)$; $\varepsilon(z)$ is the zero-mean spatial variability with standard deviation = 1. Suppose that the horizontal SOF is significantly larger than the diameter B, so that horizontal spatial variability can be ignored. The unit side resistance $f_s(z)$ is expressed as

$$f_s(z) = \alpha \cdot s_u(z) \quad (3)$$

where α = 0.5 is adopted for illustration. For a friction pile, the end bearing is negligible, so the total resistance Q_u is equal to the total shaft resistance:

$$Q_u = \pi B \int_0^L f_s(z)\,dz = \alpha \pi B L (\mu + \sigma \cdot \bar{\varepsilon}_L) \quad (4)$$

where $\bar{\varepsilon}_L$ is the spatial averaged $\varepsilon(z)$ over the depth range L. The limit state function G can be defined as

$$G = Q_u - DL = \alpha \pi B L (\mu + \sigma \cdot \bar{\varepsilon}_L) - DL \quad (5)$$

The pile fails if G < 0.

The W-M model with vertical SOF = δ and smoothness parameter = ν is adopted as the ACF model for $\varepsilon(z)$. The spatial average $\bar{\varepsilon}_L$ over the depth between 0 m and 10 m can be computed as the arithmetic average of the $\varepsilon(z)$ values simulated over the dense grid points (z_1, z_2, …, z_n). Each sample path of $\varepsilon(z)$ produces a realization of $\bar{\varepsilon}_L$, hence a realization of G. Ten thousands (N = 10,000) realizations of G are simulated, and the failure probability $p_f = P(G < 0)$ can be estimated:

$$p_f \approx \frac{1}{N} \sum_{i=1}^{N} I\left[G^i < 0\right] \quad (6)$$

where I[.] is the indicator function; G^i is the i-th realization of G. For cases with small p_f, N increases to 100,000. Figure 2 shows how p_f changes with ν for several chosen δ/L values. It is clear that ν does not significantly affect p_f, but δ/L does. This is because the limit state for the friction pile example is completely governed by spatial averaging, and the effect of spatial averaging can be summarized by the variance reduction. Therefore, ν does not significantly affect p_f.

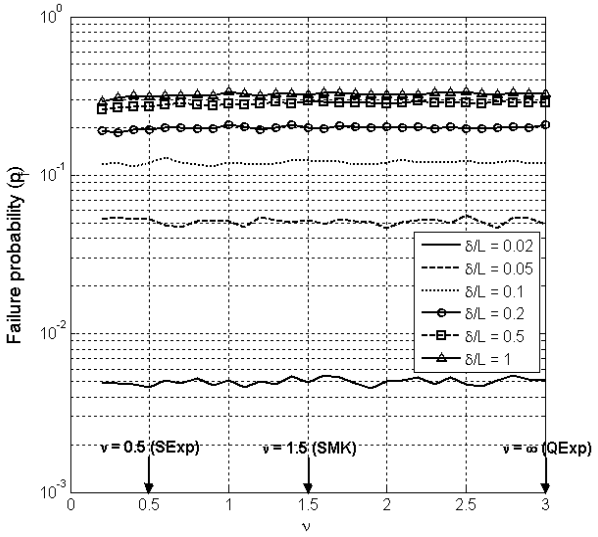

Figure 2 Variation of p_f with respect to ν for several chosen δ/L values (friction pile).

2.2. Infinite slope

Let us consider an infinite slope with an inclination angle α = 22^o and depth to bedrock = D. The direction parallel to the slope is denoted by x and that perpendicular to the slope by z. Suppose the friction angle ϕ' of the cohensionless soil is spatially variable only in the z direction and is homogeneous in the x direction. The ground water is assumed to be deep, so it has no effect on the slope stability. The spatially variable $\tan[\phi'(z)]$ is

modeled as a stationary normal random field with mean $\mu = \tan(30^o)$ and COV = 10%:

$$\tan\left[\phi'(z)\right] = \mu + \sigma \cdot \varepsilon(z) \tag{7}$$

where $\tan[\phi'(z)]$ denotes the tangent of the friction angle at depth z; $\sigma = \tan(30^o) \times 10\%$ is the standard deviation of $\tan[\phi'(z)]$; $\varepsilon(z)$ is modeled as a zero-mean stationary normal random field with standard deviation = 1.

For the infinite slope, a potential slip plane with depth z fails if $\tan[\phi'(z)] < \tan(\alpha)$, and the slope fails if any potential slip plane fails. Therefore, the limit state function G for the infinite slope can be written as

$$\begin{aligned} G &= \min_{z\in[0,10]} \tan\left[\phi'(z)\right] - \tan(\alpha) \\ &= \mu + \sigma \cdot \varepsilon_{\min} - \tan(\alpha) \end{aligned} \tag{8}$$

where ε_{min} denotes the minimum value of the $\varepsilon(z)$ sample path. The infinite slope fails if $G < 0$. Here, the weakest-path seeking mechanism governs the failure of an infinite slope, and it manifests as the minimization of $\tan[\phi'(z)]$ in Eq. (8). There is no spatial averaging in Eq. (8). The W-M model with SOF = δ and smoothness parameter = ν is adopted as the ACF model for $\varepsilon(z)$. Sample paths of $\varepsilon(z)$ are simulated using FSM. Each sample path of $\varepsilon(z)$ produces a realization of ε_{min}, hence a realization of G. Ten thousands (N = 10,000) realizations of G are simulated, and the failure probability p_f can be estimated using Eq. (6). For cases with small p_f, N increases to 100,000. Figure 3 shows how p_f changes with ν for several chosen δ/D values. It is clear that ν now has a significant effect on p_f. In particular, p_f produced by SExp ($\nu = 0.5$) is significantly larger than those produced by SMK ($\nu = 1.5$) and QExp ($\nu = \infty$) even if they share the same δ/D. This observation stands in strong contrast to that obtained in the friction pile example. For the friction pile example, spatial averaging completely governs, hence δ is the *only* parameter that matters. The parameter ν does not have much effect on p_f because ν does not have much effect on the variance reduction. On the contrary, for the infinite slope example, there is no spatial averaging, and weakest-path seeking mechanism completely governs. The local jitters produced by a small ν lead to lots of apparent weak layers that affect the stability of the infinite slope. As a result, ν has a significant effect on p_f for the infinite slope problem. The "smoothness" of the spatial variability was not well addressed in the geotechnical literature, and the "correlation length" has been the only focus. An extra parameter such as the parameter ν in the W-M model is needed to capture the "smoothness" of the spatial variability based on site investigation data.

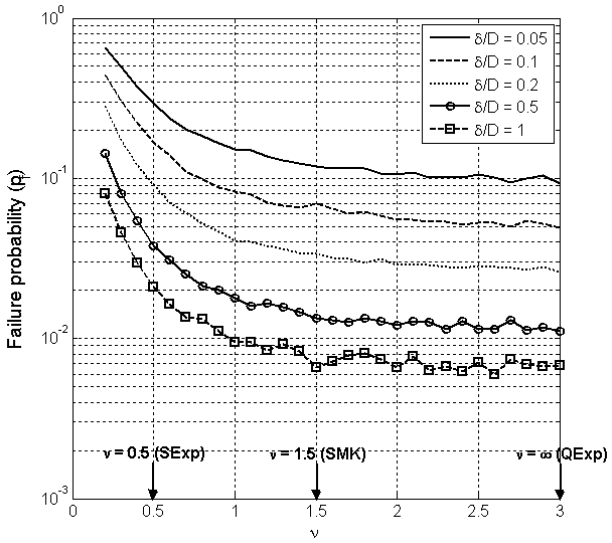

Figure 3 Variation of p_f with respect to ν for several chosen δ/D values (infinite slope).

2.3. Differential settlement between two footings

Let us consider two square rigid footings on undrained clay, with width B = 1 m and separation distance = L = 5 m. The depth of a hard stratum is assumed to be very deep. Each footing is subjected to a vertical load of Q = 200 kN, producing a bearing pressure of $q = Q/B^2 = 200$ kN/m^2. The horizontal direction is denoted by x. The Young's modulus E for the undrained clay underlying the footing is denoted by E(x). It is assumed that E(x) has taken into account the (weighted) average of E over 4B to 5B beneath the footing. The spatially variable E(x) is modeled as

a stationary lognormal random field with mean μ = 20 MN/m^2 and COV = 50%. This suggests that ln[E(x)] is a stationary normal random field with variance $\xi^2 = \ln(1+COV^2)$ mean $\lambda = \ln(\mu) - 0.5\times\xi^2$:

$$\ln\left[E(x)\right] = \lambda + \xi \cdot \varepsilon(x) \tag{9}$$

where $\varepsilon(x)$ is the zero-mean spatial variability with standard deviation = 1. The W-M model with SOF = δ and smoothness parameter = ν is adopted as the ACF model for $\varepsilon(x)$. The settlement S_e at the center of each rigid footing can be estimated as (Janbu et al. 1956; Christian and Carrier 1978)

$$S_e(x) = 0.93 \times \frac{q \cdot B}{E(x)} \times A_1 A_2 \tag{10}$$

where A_1 is a factor for the depth of hard stratum; A_2 is a factor for the embedment depth; 0.93 is the correction factor for a rigid footing (Timoshenko and Goodier 1970). For the current case, the hard stratum is deep so that $A_1 \approx 0.7$ (Christian and Carrier 1978), and there is no embedment depth so that $A_2 = 1$. The angular distortion between the two footings is denoted by β:

$$\beta = \frac{\left|S_e(x_1) - S_e(x_2)\right|}{L} \tag{11}$$

where (x_1, x_2) are the x coordinates for the two footings. The limit state function G can be written as

$$G = \frac{1}{500} - \beta \tag{12}$$

where 1/500 is the maximum acceptable angular distortion (European Committee for Standardization 1994).

Each sample path of $\varepsilon(x)$ produces a realization of E(x). $S_e(x_1)$ and $S_e(x_2)$ can be computed from $E(x_1)$ and $E(x_2)$, and a realization of angular distortion β as well as a realization of G can be computed. A hundred thousand (N = 100,000) realizations of G are simulated, and the failure probability p_f can be estimated using Eq. (6). Figure 4 shows how p_f changes with ν for several chosen δ/L values. It is clear that ν has a significant effect on p_f when δ/L is relatively large. When δ/L is large, the separation distance between the footings is only a fraction of δ. In this case, the differential settlement between the two footings is governed by the short range auto-correlation, and the short range auto-correlation behaviors for ACF models with different ν are fairly different. This explains why ν has a significant effect on p_f when δ/L is relatively large. It is noteworthy that there is no weakest-path seeking for the differential settlement problem, yet ν still has a significant effect on p_f. As a result, the significant effect of ν is not limited to cases with weakest-path seeking.

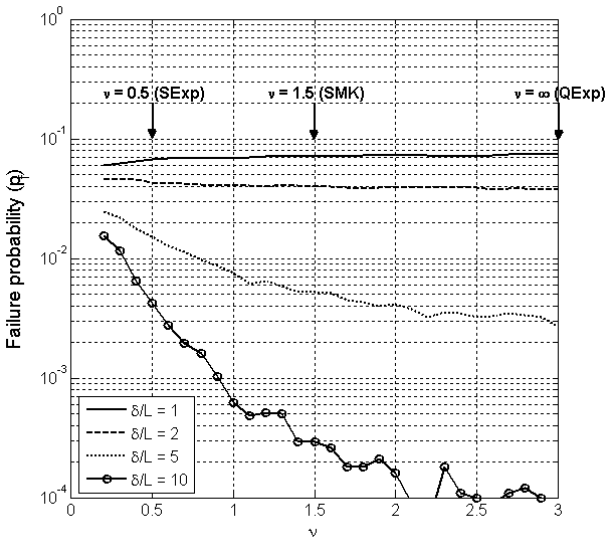

Figure 4 Variation of p_f with respect to ν for several chosen δ/L values (differential settlement).

3. CONCLUSIONS

In the geotechnical literature, the scale of fluctuation (δ) has been treated as the main (and probably the only) parameter that characterizes the auto-correlation of a spatially variable soil property. The current paper shows that ν has an insignificant effect and that δ *alone* is important if the limit state is completely governed by spatial averaging, such as the friction pile under axial compression. However, not all limit states are completely governed by spatial averaging. The

current paper shows that ν has a significant effect when the weakest-path seeking mechanism is important (e.g., infinite slope). For serviceability limit state problems with spatially variable modulus, the angular distortion between footings is considered in the current paper, and it involves taking the spatial difference, which is *not* the same as spatial averaging. The current paper shows that ν has a significant effect on p_f as well. The practical conclusion of this paper is that characterizing and modeling the scale of fluctuation alone may be insufficient for the purpose of reliability analysis. Besides characterizing and modeling the scale of fluctuation, it is more prudent to also characterize and model the smoothness of the spatial variability.

4. ACKNOWLEDGEMENTS

The authors would like to thank Dr. Yu-Gang Hu and Miss Tzu-Ting Lin for their efforts in producing the results in some plots.

5. REFERENCES

Abramowitz, M. and Stegun, I. (1970). Handbook of Mathematical Functions. Dover, New York.

Ching, J. and Sung, S.P. (2016). Spatial averaging of stationary random fields along curves – simulation and variance reduction, Journal of GeoEngineering, 11(1), 33-43.

Ching, J., Phoon, K.K., Beck, J.L., and Huang, Y. (2017a). On the identification of geotechnical site-specific trend function, ASCE-ASME Journal of Risk and Uncertainty in Engineering Systems, Part A: Civil Engineering, 3(4), 04017021.

Ching, J., Wu, T.J., Stuedlein, A.W., and Bong, T. (2017b). Estimating horizontal scale of fluctuation with limited CPT soundings. Geoscience Frontiers, 9, 1597-1608.

Christian, J.T. and Carrier, W.D. (1978). Janbu, Bjerrum, and Kjaernsli's chart reinterpreted. Canadian Geotechnical Journal, 15, 124-128.

European Committee for Standardization (1994). Geotechnical Design, General Rules – Part 1, Eurocode 7. Brussels, Belgium.

Guttorp, P. and Gneiting, T. (2006). Studies in the history of probability and statistics XLIX on the Matérn correlation family. Biometrika, 93(4), 989-995.

Janbu, N., Bjerrum, L., and Kjaernsli, B. (1956). Veiledning vedlosning av fundamentering – soppgaver. Publication No. 18, Norwegian Geotechnical Institute, 30-32.

Jha, S.K. and Ching, J. (2013). Simulating spatial averages of stationary random field using Fourier series method. ASCE Journal of Engineering Mechanics, 139(5), 594-605.

Liu, W.F., Leung, Y.F., and Lo, M.K. (2017). Integrated framework for characterization of spatial variability of geological profiles. Canadian Geotechnical Journal, 54(1), 47-58.

Rasmussen, C.E. and Williams, C.K.I. (2006). Gaussian Processes for Machine Learning, the MIT Press.

Stein, M.L. (1999). Interpolation of Spatial Data: Some Theory for Kriging. Springer, New York.

Timoshenko, S. and Goodier, J.N. (1970). Theory of Elasticity. 3rd ed. McGraw Hill, New York.

Vanmarcke, E.H. (1977). Probabilistic modeling of soil profiles. ASCE Journal of Geotechnical Engineering, GT11, 1227-1246.

Vanmarcke, E.H. (1983). Random Fields: Analysis and Synthesis. The MIT Press, Cambridge, Massachusetts.